Research article

X-RAY SPECTROMETRY

Received: 28 September 2016 Revised: 24 January 2017 Accepted: 6 February 2017 Published online in Wiley Online Library

(wileyonlinelibrary.com) DOI 10.1002/xrs.2762

Synthesis, chemical and microstructural characterization of micro macroporous biphasic calcium phosphate granules

M. A. Garcés Villalá,[a,b] J. L. Calvo Guirado,[c] D. Granados,[b] S. P. Limandri[d,e] and V. Galván Josa[d,e]*

A route based on calcium phosphate emulsions with addition of glycolic acid as pore former was developed for synthesizing porous nanocrystalline biphasic calcium phosphate ceramics. The method is low cost and gives a biphasic calcium phosphate composed of 88% β-tricalcium phosphate and 12% hydroxyapatite. The material obtained is characterized by scanning electron microscopy, X-ray diffraction and X-ray fluorescence techniques, and the specific surface area is determined by the Brunauer, Emmett and Teller method. The small crystalline domain sizes obtained (68 and 87 nm for β-tricalcium phosphate and hydroxyapatite phases, respectively) allow a major contact reaction and stability in the interphase between the implanted material and natural bone, as well as a better promotion effect on the early bone in-growth. The improvement of the physical, chemical and structural properties by the balanced combination of the ceramic phases, the small crystallite size, the high porosity and high specific surface area obtained is a desirable characteristic in bone tissue engineering and encourages the performance of animal studies *in vivo* to evaluate their use for applications such as bone replacement in humans.

Introduction

Tissue engineering is an interdisciplinary field in which engineering and life science principles are combined to obtain biological substitutes capable of restoring, keeping or improving the function of the tissue or organ that has been affected. To be accepted as a bone matrix, a material must fulfill certain requirements related to biocompatibility, osteoconduction, osteointegration and bioabsorbabilty, and it must also have suitable mechanical properties to provide structural support during bone growth, allowing vascular neoproliferation and consequently osteogenesis. Several *in vivo* and *in vitro* experiments have shown that calcium phosphates in many forms (porous blocks, coatings and powders, among others) and phases (crystalline, amorphous or mixtures) support the attachment, differentiation and proliferation of cells (such as osteoblasts and mesenchymal cells).[1] They are mainly used as bone grafting materials and, due to their high hygroscopicity, as drug delivery systems.[2]

The biphasic calcium phosphates (BCPs), which are composed of a stable phase, hydroxyapatite (HA) ($Ca_{10}(PO_4)_6(OH)_2$, HA) and a more soluble phase, generally β-tricalcium phosphate ($Ca_3(PO_4)_2$, BTCP), present several advantages over the single-phase components or other calcium phosphate ceramics because of their unique dissolution characteristics promoting new bone formation at the implant site.[3] Medical applications of BCP are currently focused on the production of non-load-bearing implants, such as bone graft substitutes in oral or orthopedic surgery, or as coating for implants.[4]

Biphasic calcium phosphate can be obtained by sintering biologic or synthetic apatites. Sintering commercial calcium phosphate reagents above 900 °C also gives, depending on the starting material and sintering conditions, pure HA, BTCP or BCP. Another possibility to obtain BCP is by mechanically mixing two types of synthetic apatites: one resulting in BTCP and the other in HA after sintering at temperatures above 900 °C.[5]

Chemical and clinical performance of BCP is related to their stoichiometry, crystallinity and morphology.[6] The mass proportion between HA and BTPC influences the reactivity: The lower the HA/BTCP ratio, the higher the reactivity.[7] Mechanical properties are associated with the Ca/P molar fraction.[8] Bioactivity and osteoconduction are associated with the material solubility, which increases when some Ca atoms are substituted by Sr.[9] Regarding this last effect, the incorporation of chemical species into the apatite structure influences the physical, chemical and physiological properties of the solid and consequently affects the mineralization

* *Correspondence to: Victor Galván Josa, Facultad de Matemática Astronomía y Física, Universidad Nacional de Córdoba, Medina Allende s/n, Ciudad Universitaria, 5016 Córdoba, Argentina. E-mail: galvan@famaf.unc.edu.ar*

a *Facultad de Odontología, Universidad Nacional de Córdoba, Haya de la Torre s/n Ciudad Universitaria, 5016, Córdoba, Argentina*

b *Instituto de Ingeniería Química, Universidad Nacional de San Juan, Libertador San Martín 1109, 5400, San Juan, Argentina*

c *Universidad Católica San Antonio de Murcia, Campus de los Jerónimos 135, Guadalupe, 30107, Murcia, Spain*

d *Facultad de Matemática Astronomía y Física, Universidad Nacional de Córdoba, Medina Allende s/n, Ciudad Universitaria, 5016, Córdoba, Argentina*

e *Instituto de Física Enrique Gaviola, CONICET, Buenos Aires, Argentina*

process of the calcified tissues.[10–12] Mg substitution has its own significance in the calcification process and on bone fragility and has an indirect influence on mineral metabolism.[3,10] Besides, it also influences the apatite crystallization, promoting the formation of BTCP.[13] The presence of Na in biological apatites plays an important role in the cell adhesion and also in bone metabolism and resorption processes.[3] Trace Zn amounts favor osteoblastic cell proliferation and differentiation, adding a potent and selective inhibitory effect on osteoclastic bone resorption *in vitro*.[12]- The beneficial effects of Sr arise from its capacity to prevent bone loss by depressing bone resorption and maintaining bone formation.[14]

Structural and morphological properties also affect the bioceramic performance. For dentistry applications, a high specific surface area is usually desired in order to maximize the interaction of multinucleated cells with the bone substitute.[15] Optimum granule morphology ensures an adequate space for new vascular sprouts and the consequent invasion by osteoprogenitor cells. The 3D array of the granules is another factor that has received low attention, despite its potential effect on osteoconduction.[16] Calcium phosphate scaffolds with macro (>50 μm) and micro (<10 μm) pores produce capillary forces allowing adhesion and penetration of cells.[17] A macroporous structure favors cell ingrowth and blood vessel invasion[18] because of the similarity between the pore size and the macroporosities in human spongy bone.[19] Microporosity allows the entrapment and concentration of proteins, which, when contact with undifferentiated cells, induce their differentiation.[20,21]

The aim of this work is to present a fast and low-cost sintering process to obtain BCP granules with optimal chemical, mineralogical and morphological characteristics for grafting purposes in oral surgery. The chemical and structural characterization performed here is the first step for obtaining a biocompatible material. *In vivo* animal tests, which are not covered in the present study, constitute the following step necessary to evaluate the tissue responses to the implanted material.

Materials and methods

Synthesis

Biphasic calcium phosphate powder was obtained by using a technical grade mixture of calcium phosphates (60% HA, 30% calcium hydrogen phosphate and 10% tricalcium phosphate) and an aqueous solution of glycolic acid $C_2H_4O_3$ at 70% with pH = 0.35 (Sigma-Aldrich). The last compound is diluted at 50% in water, adjusting its pH value to 0.7. The liquid glycolic acid is added to the powder at a proportion of 1 ml/g in a glass vessel and continuously stirred at 60 rpm in a stainless steel mixer for 2 min. An exothermic reaction with a maximum temperature of 54.5 °C is produced. Then, to evaporate the water excess, the sample is dried in a furnace at 100 °C for 24 h. The material obtained is ground to break up agglomerates and sieved to obtain particle sizes of 500–1000 μm. After that, the sample is heated at 600 °C for 10 min under a 60 °C/min heating rate at atmospheric pressure. Afterwards, the temperature is raised (with the same heating rate) until 1100 °C is reached, and the material is maintained at this temperature for 6 h in vacuum atmosphere. This last thermal treatment produces a solid-state reaction that reduces 53% of the sample weight and transforms the material into crystalline BTCP and HA. The new material is sieved again with the same sieved size previously used.

Characterization techniques

The morphology and microstructure of the final particles obtained were observed from secondary electron images, acquired in a Field Emission Scanning Electron Microscope (FE-SEM) Σigma Zeiss electron microscope, operated at 5 kV. To this aim, final granules were dispersed in carbon tapes and sputtered with 10-nm-thick chromium layers.

The chemical composition was determined by X-ray fluorescence (XRF); a total of five fusion beads were prepared in order to get reproducible results with a Claisse M4 flux-litetetraborate–dilithium tetraborate ($Li_2B_4O_7$) (Claisse, Canada). For each fusion bead, 1 g of sample and 8 g of flux were weighed (with an accuracy of 0.0001 g) and put into a previously cleaned crucible. The use of fusion beads has several advantages over the conventional press pellets, such as as elimination of particle size and structure effects, removement of the heterogeneity, decrease of interelement influence and lower consumption of the sample, which leads to more accurate results. The measurements were performed in an XRF sequential spectrometer Bruker F8 Tiger. The X-ray tube has a Rh anode, and the characteristic X-ray lines were detected with LiF(200) (K-U), PET (Al-Cl) and XS-55 (O-Mg) crystals and with a proportional counter (for low *Z* elements) and a scintillator counter (for high *Z* elements).

The specific surface area was determined by the triple-point Brunauer, Emmett and Teller (BET) method.[22] The sample was dried and degassed at 400 °C for 2 h. Three independent measurements were carried out in a DigiSorb 2600 micromeritics surface area analyzer, and krypton gas was used as adsorbate, because the value obtained for BET area by using nitrogen gas is below the precision limit of the equipment.

A PANalytical Empyrean Philips PW 3710 X-ray diffractometer was used to determine the mineral phases present in the raw material used and in the final sample. Five independent measurements were performed for each sample in the interval 5–90 ° 2θ with a step size of 0.02 °, Cu-Kα radiation, 30 kV voltage and 25 mA current. Rietveld refinements were carried out in order to determine the mineral mass concentrations and the Ca substitution by Mg in the BTCP phase. The results presented here correspond to the mean values of the independent measurements.

The Rietveld method

The Rietveld method is a suitable alternative for the quantitative analysis of mixtures of polycrystalline phases. It uses a least squares approach to refine a theoretical X-ray diffraction pattern until it matches the measured profile.[23] The model for the calculated profile includes structural (spatial group, atoms in the asymmetric unit, temperature factors etc.), microstructural (concentration, crystal size and microdeformation) and instrumental (slit width, sample size etc.) factors.

In this work, the software TOPAS 3® with fundamental parameters approach was used for the Rietveld refinements. The parameters refined were the background, which was modelled by sixth-order Chebyshev polynomial, the sample displacement, the zero correction, the crystallite sizes of HA and BTCP phases and some Ca occupancy factors for the BTCP structure. The International Crystal Structure Database (ICSD) codes used as starting crystallographic data for HA and BTCP were #22059 and #410782, respectively. Temperature factors were not refined, because their influence is negligible compared with the statistical uncertainties and the errors associated with the refinement of occupancy factors.

In order to provide a figure of merit for the performance of the fit, the goodness of fit is assessed through the weighted comparison of the predicted intensities Y' with the experimental ones Y:

$$\mathrm{GOF} = \sqrt{\frac{1}{N-P}\sum_{i=1}^{N}\frac{\left(Y_i - Y_i'\right)^2}{Y_i}} \quad (1)$$

where i denotes each of the N channels in the considered XRD pattern and P is the number of refined parameters.[23] The statistical quality of the fit is represented by the R_e value, defined as follows:

$$R_e = \sqrt{\frac{N-P}{\sum_{i=1}^{N} Y_i}} \quad (2)$$

Results and discussion

The physical structure of BCP sample obtained in this work can be observed in the SEM micrographs (Fig. 1) acquired at different magnifications. The presence of porous with sizes ranging from 50 to 200 μm (macropores) is evidenced in Fig. 1(a) and (b). Particles bear irregular shapes with rounded borders, which is associated with a high macroporosity. The particle surface is mainly concave, which is advantageous because this surface morphology favors cell adhesion and proliferation and it is responsible for the beginning of new bone formation.[24]

The particle microstructure consists in a highly porous agglomerate of fine micrometer-sized grains [Fig. 1(c) and (d)]. The mean diameter of these subunits is 1.5 ± 1.0 μm, and their irregular morphology indicates that they are not completely coherent crystalline domains. The necking among the grains is due to the final sintering temperature at 1000 °C.[25] The total volume associated with the micrometric pores, obtained from the images acquired at the same magnification (3500×) for different particles, resulted at around 35%. This is only a rough estimation because images do not correspond to a flat sample and the precise delimitation of pores is not straightforward.

The specific surface area of the material studied, obtained by the BET method, is 4.06 ± 0.06 m^2/g, which lies between the largest values reported in literature for the sintering temperatures used in this work. For instance, Gauthier *et al.*[5] reported BET areas of 3.5–3.9 m^2/g for BCP with 60/40 HA/BTCP ratio, whereas Descamps *et al.*[15] obtained areas ranging from 2.5 to 5 m^2/g for pure BTCP at calcination temperatures of 950 °C. The high porosity observed in SEM images and high surface area obtained can be associated with the effect of the glycolic acid in the sintering process. As it was mentioned in the introduction, a large surface area (closely related with microporosity) is necessary to achieve excellent osteoconductivity and to promote material resorption.[26]

The average mass concentrations obtained by XRF for the sample synthetized and for natural bone are shown in Table 1. The natural bone composition was estimated by renormalization of data given by Kannan *et al.*[3] removing the carbonate groups and constitutes a rough approximation, because there are strong variations in major and trace elements according to age, nutrition and bone type. The mass concentration uncertainties were estimated by quantifying a fusion bead of an HA purum p.a. sample (Sigma-Aldrich), resulting at around 0.01% for all the elements studied. The low uncertainty values obtained are related to the use of fusion beads for the XRF measurements, which minimizes matrix effects and leads to more accurate results. The presence of Na, Mg, Sr, Ni and Zn as minor and trace elements is expectable and can be associated with impurities of the raw materials used. It is well known that ionic components Ca^{2+} and (PO_4) in calcium phosphates can be easily interchanged by other ions;[3] particularly, some Ca sites are naturally substituted by Sr and Mg. As it was previously mentioned, the presence of these trace elements is not negative, because some ionic substitutions favor physical, chemical and physiological properties of bioceramics. It is important to mention that Ti and Al were not detected in the samples obtained here. These elements negatively affect solubility properties and mineralization processes. Mass concentrations higher than 1 and 7 for TiO_2

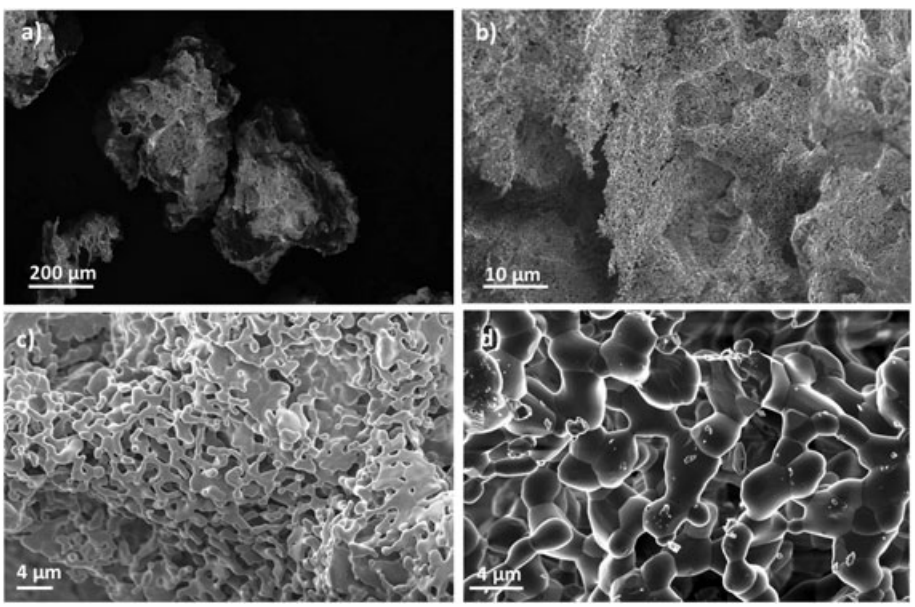

Figure 1. SEM micrographs corresponding to one of the biphasic calcium phosphate granules acquired at (a) 50×, (b) 500×, (c) 2000× and (d) 3500×.

Table 1. Mass concentrations obtained by X-ray fluorescence for the BCP sample obtained here

Element	Composition wt%	
	Bone	BCP
Ca	37.6	37.98
P	16.4	19.77
Na	0.97	0.76
K	0.78	—
F	0.03	—
Cl	0.14	—
Sr	—	0.03
Zn	—	0.008
Ni	—	0.008
Ca/P molar ratio	1.71	1.48

The results correspond to the mean value of five independent measurements, and the estimated uncertainties are lower than 0.01% (as described in the text). The natural bone composition[3] is also shown as comparison.

BCP, biphasic calcium phosphate.

and Al_2O_3 respectively extend the time necessary to achieve the material bone connection.[27]

The X-ray diffraction patterns and the fits obtained by Rietveld refinement corresponding to the final sample and to the raw material used are shown in Fig. 2. The fits are acceptable according to the resulting goodness-of-fit and R_e factors. The phase concentration

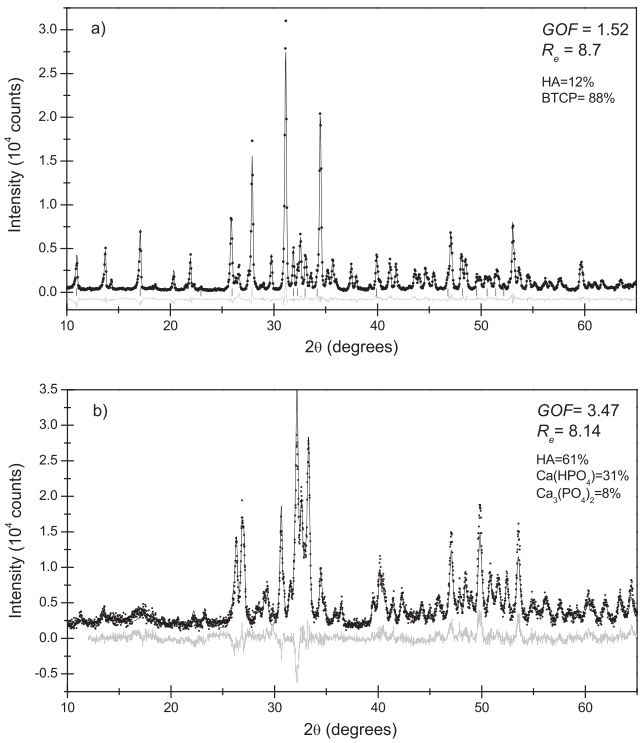

Figure 2. Rietveld analysis patterns of powder diffraction data of the (a) biphasic calcium phosphate (BCP) sample obtained and (b) calcium phosphate mixture used as precursor in this work. Dots: measured profile; black line: calculated profile; and gray line: residue. The most intense peaks corresponding to the hydroxyapatite (HA) phase in the BCP sample are marked below the profile with vertical bars. GOF, goodness of fit; BTCP, β-tricalcium phosphate.

obtained for the raw material is HA 61%, dicalcium phosphate 31% and BTCP 8%, which is in good agreement with the nominal composition. The corresponding domain sizes are 29, 50 and 32 nm, respectively. Regarding the final BCP granules obtained, only HA and BTCP phases were detected, with mass percentage contents of 12% and 88%, respectively; this proportion is advantageous, because bone induction occurs fastest for BCP with HA/BTCP ratios of around 20/80 and 15/85, compared with pure HA, BTCP or BCP with higher HA/BTCP values.[28,29]

The lattice parameters obtained for the BTCP phase are $a = b = 10.435$ Å and $c = 37.418$ Å, which are barely lower than the cell parameters corresponding to BTCP without Mg substitution ($a = b = 10.4352$ Å and $c = 37.4029$ Å).[30] This contraction in the cell parameters is associated with the Ca substitution by Mg, which has a lower ionic radius.[31] Bearing in mind that BTCP crystallizes into the rhombohedral space group R3c with five crystallographically independent sites for calcium, and considering that the maximum substitution occurs at the Ca(5) site,[31] it is possible to obtain the amount of Ca substitution from the Rietveld analysis by refining the Ca(5) occupancy. We obtained that 15% of the Ca(5) site is occupied by Mg atoms in the studied sample, which implies a presence of around 0.01% of Mg in the sample. This value reasonably agrees with the results obtained by XRF.

The crystalline domain sizes obtained from the refinement are 68 and 87 nm for BTCP and HA phases, respectively. Small crystal domains are desirable because they allow a major contact reaction and stability in the interphase between the implanted material and natural bone, as well as a better promotion effect on the early bone in-growth.[32]

The crystallinity X_c grade corresponding to the fraction of crystalline phases is 99% and was evaluated according to the relation [33]:

$$X_c = \frac{1 - Back_{(300)-(0\,2\,10)}}{I_{(0\,2\,10)}} \tag{3}$$

where $Back_{(300)\ -\ (0\ 2\ 10)}$ is the background intensity between (300) and (0 2 10) BTCP reflections and $I_{(2\ 0\ 10)}$ is the intensity of the maximum peak, corresponding to the (2 0 10) reflection.

The total porosity can be calculated by comparing the theoretical density ρ_c of an HA-BCTP mixture with the measured density ρ_m. Assuming the mass concentrations C_{HA} and C_{BTCP} obtained by XRD for HA and BCTP phases, respectively, and using the theoretical densities of each phase ($\rho_{HA} = 3.156$ g/cm^3 and $\rho_{BTCP} = 3.07$ g/cm^3), ρ_c is estimated as follows:

$$\rho_c = \left(\frac{C_{HA}}{\rho_{HA}} + \frac{C_{BTCP}}{\rho_{BTCP}}\right)^{-1} = 3.11^{g}/_{cm^3} \tag{4}$$

The value ρ_m was determined by weighing a known material volume in a high-precision scale, resulting in 0.55 g/cm^3. The total pore volume is, thus, as follows:

$$V_p = M\left(\frac{1}{\rho_m} - \frac{1}{\rho_c}\right) \tag{5}$$

and the porosity is as follows:

$$P = \frac{V_p}{V_T} \tag{6}$$

where V_T is the total sample volume. The porosity obtained with Eqns (4)–(6) is 82%.

The same method was applied by Li *et al.*[33] for two commercial samples resulting in values of 75% and 80%. Porosity of 79%

(measured by the Archimedes method) was reported by Amera *et al.*[29] for a 16/84 HA/BTCP sample.

Conclusions

A new process for sintering BCP ceramics (HA + BTCP) is presented. A technical grade (low-cost) mixture of calcium phosphates is used as precursor and glycolic acid as pore former. Improvement of the structural properties by the balanced combination of the ceramic phases was achieved in this nanocrystalline material, which has 12% HA and 88% BTCP. The high values obtained for the specific surface area (4.06 m^2/g) and porosity (82%), as well as the particle structure, suggest that this material is suitable for bone grafting applications in oral surgery. *In vivo* animal experimentation involving the implantation in bone of the material presented in this work is currently being carried out in order to evaluate osteointegration properties.

Acknowledgements

The authors gratefully acknowledge the *Laboratorio de Microscopía Electrónica y Análisis por Técnicas de Rayos X* (LAMARX) and the *Centro AtómicoBariloche*, where measurements were carried out. Financial support from the *Consejo Nacional de Investigaciones Científicas y Técnicas* and the *Secretaría de Ciencia y Técnica* of the *Universidad Nacional de Córdoba* of the Argentine Republic is also acknowledged.

References

[1] J. R. Jones, L. L. Hench. Materials perspective. Biomedical materials for new millennium: perspective on the future. *Mater Sci Technol* **2001**, *17*, 891–900.
[2] S. S. Syamchand, G. Sony. Multifunctional hydroxyapatite nanoparticles for drug delivery and multimodal molecular imaging. *Microsc Acta* **2015**, *182*, 1567–1589.
[3] S. Kannan, F. Goetz-Neunhoeffer, J. Neubauer, J. M. F. Ferreira. Ionic substitutions in biphasic hydroxyapatite and β-tricalcium phosphate mixtures: structural analysis by Rietveld refinement. *J Am Ceram Soc* **2008**, *91*, 1–12.
[4] R. Z. Legeros, S. Lin, R. Rohanizadeh, D. Mijares, P. Legeros. Biphasic calcium phosphate bioceramics: preparation, properties and applications. *J Mater Sci Mater Med* **2003**, *14*, 201–209.
[5] O. Gauthier, L. M. Bouler, E. Aguado, R. Z. Legeros, P. Pilet, G. Daculsi. Elaboration conditions influence physicochemical properties and *in vivo* bioactivity of macroporous biphasic calcium phosphate ceramics. *J Mater Sci Mater Med* **1999**, *10*, 199–204.
[6] S. Meejoo, W. Maneeprakorn, P. Winotai. Phase and thermal stability of nanocrystalline hydroxyapatite prepared via microwave heating. *Thermochemical Acta* **2006**, *447*, 115–120.
[7] G. Daculsi, O. Laboux, O. Malard, P. Weiss. Current state of the art of biphasic calcium phosphate bioceramics. *J Mater Sci Mater Med* **2003**, *14*, 195–200.
[8] S. Raynaud, E. Champiom, J. P. Lafon, D. Bernache-Assollant. Calcium phosphate apatites with variable Ca/P atomic ratio III. Mechanical properties and degradation in solution of hot pressed ceramics. *Biomaterials* **2002**, *23*, 1081–1089.
[9] M. Roy, G. A. Fielding, A. Bandyopadhyay, S. Bose. Effects of zinc and strontium substitution in tricalcium phosphate on osteoclast differentiation and resorption. *Biomater Sci* **2013**, *1*, 74–82.
[10] A. Bigi, E. Foresti, M. Gandolfi, M. Gazzano, N. Roveri. Isomorphous substitutions in betatricalcium phosphate: the different effects of zinc and strontium. *J Inorg Biochem* **1997**, *66*, 259–265.
[11] W. Suchanek, K. Byrappa, P. Shuk, R. Riman, V. Janas, K. S. TenHuisen. Mechanochemical hydrothermal synthesis of calcium phosphate powders with coupled magnesium and carbonate substitution. *J Sol St Chem* **2004**, *177*, 793–799.
[12] X. Li, Y. Sogo, A. Ito, H. Mutsuzaki, N. Ochiai, T. Kobayashi. The optimum zinc content in set calcium phosphate cement for promoting bone formation in vivo. *Mater Sci Eng* **2008**, *29*, 969–975.
[13] P. Kanchana, C. Sekar. Effect of magnesium on the mechanical and bioactive properties of biphasic calcium phosphate. *J Min Mat Char Eng* **2012**, *11*, 982–988.
[14] P. Marie, P. Ammann, G. Boivin, C. Rey. Mechanisms of action and therapeutic potential of strontium in bone. *Calcif Tissue Int* **2001**, *69*, 121–129.
[15] M. Descamps, J. Hornez, A. Leriche. Effects of powder stoichiometry on the sintering of β-tricalcium phosphate. *J Eur Ceram Soc* **2007**, *27*, 2401–2406.
[16] D. Chappard, B. Guillaume, R. Mallet, F. Pascaretti-Grizon, M. F. Basle, H. Libouban. Sinus lift augmentation and b-TCP: a microCT and histologic analysis on human bone biopsies. *Micron* **2010**, *41*, 321–326.
[17] S. J. Polak, L. E. Rustom, G. M. Genin, M. Talcott, A. J. Wagoner Johnson. A mechanism for effective cell-seeding in rigid, microporous substrates. *Acta Biomater* **2013**, *9*, 7977–7986.
[18] M. C. Doernberg, B. von Rechenberg, M. Bohner, S. Grunenefelder, G. An Lenthe, R. Muller, B. Gasser, R. Mathys, G. Baroud, J. Auer. In vivo behavior of calcium phosphate scaffolds with four different pore sizes. *Biomaterials* **2006**, *27*, 5186–5198.
[19] R. LeGeros. Calcium phosphate materials in restorative dentistry: a review. *Adv Dent Res* **1988**, *2*, 164–180.
[20] O. Chan, M. J. Coathup, A. Nesbitt, C. Y. Ho, K. A. Hing, T. Buckland, C. Campion, G. W. Blunn. The effects of microporosity on osteoinduction of calcium phosphate bone graft substitute biomaterials. *Acta Biomater* **2012**, *8*, 2788–2794.
[21] K. A. Hing, B. Annaz, S. Saeed, P. A. Revell, T. Buckland. Microporosity enhances bioactivity of synthetic bone graft substitutes. *J Mater Sci Mater Med* **2005**, *16*, 467–475.
[22] S. Brunauer, P. H. Emmett, E. Teller. Adsorption of gases in multimolecular layers. *J Am Chem Soc* **1938**, *60*, 309–319.
[23] R. Young*The Rietveld Method, International Union of Crystallography*, Oxford University Press, Oxford, **1993**.
[24] A. Graziano, R. Daquino, M. G. Cusella de Angelis, F. De Francesco, A. Giordano, G. Laino, A. Piattelli, T. Traini, A. De Rosa, G. Papaccio. Scaffold's surface geometry significantly affects human stem cell bone tissue engineering. *J Cell Physiol* **2008**, *214*, 166–172.
[25] S. Kwon, Y. Jun, S. Hong, H. Kim. Synthesis and dissolution behaviour of βTCP and HA/βTCP composite powders. *J Eur Ceram Soc* **2003**, *23*, 1039–1045.
[26] H. R. Ramay, M. Zhang. Preparation of porous hydroxyapatite scaffolds by combination of the gel-casting and polymer sponge methods. *Biomaterials* **2003**, *24*, 3293–3302.
[27] U. M. Gross, V. Strunz. The anchoring of glass ceramics of different solubility in the femur of the rat. *J Biomed Mater Res* **1980**, *14*, 607–618.
[28] T. Livingston Arinzeh, T. Tran, J. Mcalary, G. Daculsi. A comparative study of biphasic calcium phosphate ceramics for human mesenchymal stem-cell induced bone formation. *Biomaterials* **2005**, *26*, 3631–3638.
[29] A. Amera, A. M. A. Abudalazez, A. Rashid Ismail, N. Hayati AbdRazak, S. Malik Masudi, S. Rizal Rizal Kasim, Z. Arifin Ahmad. Synthesis and characterization of porous biphasic calcium phosphate scaffold from different porogens for possible bones tissue engineering applications. *Sci Sinter* **2011**, *43*, 183–192.
[30] M. Yashima, A. S. Takashi Kamiyama, A. J. Hoshikawa. Crystal structure analysis of β-tricalcium phosphate $Ca_3(PO_4)_2$ by neutron powder diffraction. *Sol State Chem* **2003**, *175*, 272–277.
[31] J. C. Araújo, M. S. Sader, E. L. Moreira, V. C. A. Moraes, R. Z. LeGeros, G. A. Soares. Maximum substitution of magnesium for calcium sites in Mg-BTCP structure determined by X-ray powder diffraction with the Rietveld refinement. *Mater Chem Phys* **2009**, *118*, 337–340.
[32] T. J. Webster, C. Ergun, R. H. Doremus, R. W. Siegel, R. Bizios. Enhanced functions of osteoblasts on nanophase ceramics. *Biomaterials* **2000**, *21*, 1803–1810.
[33] X. Li, Y. Sogo, A. Ito, H. Mutsuzaki, N. Ochiai, T. Kobayashi. The optimum zinc content in set calcium phosphate cement for promoting bone formation in vivo. *Mater Sci Eng* **2008**, *29*, 969–975.